

Recent results and prospects of the NA62 experiment at CERN

Sergei Kholodenko* on behalf of the NA62 Collaboration

INFN-Pisa,

56127, 3C Largo Bruno Pontecorvo, Pisa, Italy

E-mail: sergey.kholodenko@cern.ch

[†]The NA62 Collaboration: A. Akmete, R. Aliberti, F. Ambrosino, R. Ammendola, B. Angelucci, A. Antonelli, G. Anzivino, R. Arcidiacono, T. Bache, A. Baeva, D. Baigarashev, L. Bandiera, M. Barbanera, J. Bernhard, A. Biagioni, L. Bician, C. Biino, A. Bizzeti, T. Blazek, B. Bloch-Devaux, P. Boboc, V. Bonaiuto, M. Boretto, M. Bragadireanu, A. Briano Olvera, D. Britton, F. Brizioli, M.B. Brunetti, D. Bryman, F. Bucci, T. Capussela, J. Carmignani, A. Ceccucci, P. Cenci, V. Cerny, C. Cerri, B. Checcucci, A. Conovaloff, P. Cooper, E. Cortina Gil, M. Corvino, F. Costantini, A. Cotta Ramusino, D. Coward, P. Cretaro, G. D'Agostini, J. Dainton, P. Dalpiaz, H. Danielsson, M. D'Errico, N. De Simone, D. Di Filippo, L. DiLella, N. Doble, B. Dobrich, F. Duval, V. Duk, D. Emelyanov, J. Engelfried, T. Enik, N. Estrada-Tristan, V. Falaleev, R. Fantechi, V. Fascianelli, L. Federici, S. Fedotov, A. Filippi, R. Fiorenza, M. Fiorini, O. Frezza, J. Fry, J. Fu, A. Fucci, L. Fulton, E. Gamberini, L. Gatignon, G. Georgiev, S. Ghinescu, A. Gianoli, M. Giorgi, S. Giudici, F. Gonnella, K. Gorshanov, E. Goudzovski, C. Graham, R. Guida, E. Gushchin, F. Hahn, H. Heath, J. Henshaw, Z. Hives, E.B. Holzer, T. Husek, O. Hutanu, D. Hutchcroft, L. Iacobuzio, E. Iacopini, E. Imbergamo, B. Jenninger, J. Jerhot, R.W. Jones, K. Kampf, V. Kekelidze, D. Kerebay, S. Kholodenko, G. Khoriauli, A. Khotyantsev, A. Kleimenova, A. Korotkova, M. Koval, V. Kozhuharov, Z. Kucerova, Y. Kudenko, J. Kunze, V. Kurochka, V. Kurshetsov, G. Lanfranchi, G. Lamanna, E. Lari, G. Latino, P. Laycock, C. Lazzeroni, M. Lenti, G. Lehmann Miotto, E. Leonardi, P. Lichard, L. Litov, P. LoChiato, R. Lollini, D. Lomidze, A. Lonardo, P. Lubrano, M. Lupi, N. Lurkin, D. Madigozhin, I. Mannelli, A. Mapelli, F. Marchetto, R. Marchevski, S. Martellotti, P. Massarotti, K. Massri, E. Maurice, A. Mazzolari, M. Medvedeva, A. Mefodev, E. Menichetti, E. Migliore, E. Minucci, M. Mirra, M. Misheva, N. Molokanova, M. Moulson, S. Movchan, M. Napolitano, I. Neri, F. Newson, A. Norton, M. Noy, T. Numao, V. Obraztsov, A. Okhotnikov, A. Ostankov, S. Padolski, R. Page, V. Palladino, I. Panichi, A. Parenti, C. Parkinson, E. Pedreschi, M. Pepe, M. Perrin-Terrin, L. Peruzzo, P. Petrov, Y. Petrov, F. Petrucci, R. Piandani, M. Piccini, J. Pinzino, I. Polenkevich, L. Pontisso, Yu. Potrebenikov, D. Protopopescu, M. Raggi, M. Reyes Santos, M. Romagnoni, A. Romano, P. Rubin, G. Ruggiero, V. Ryjov, A. Sadovsky, A. Salamon, C. Santoni, G. Saracino, F. Sargeni, S. Schuchmann, V. Semenov, A. Sergi, A. Shaikhiev, S. Shkarovskiy, M. Soldani, D. Soldi, M. Sozzi, T. Spadaro, F. Spinella, A. Sturgess, V. Sugonyaev, J. Swallow, A. Sytov, G. Tinti, A. Tomczak, S. Trilov, M. Turisini, P. Valente, B. Velghe, S. Venditti, P. Vicini, R. Volpe, M. Vormstein, H. Wahl, R. Wanke, V. Wong, B. Wrona, O. Yushchenko, M. Zamkovsky, A. Zinchenko.

*Speaker

The NA62 experiment at CERN collected the world's largest dataset of charged kaon decays in 2016–2018, leading to the first measurement of the branching ratio of the ultra-rare $K^+ \rightarrow \pi^+ \nu \bar{\nu}$ decay, based on 20 candidates. Rare kaon decays are among the most sensitive probes of both heavy and light new physics beyond the Standard Model description thanks to the high precision of the Standard Model predictions, the availability of very large datasets, and the relatively simple decay topologies.

The NA62 experiment at CERN is a multi-purpose high-intensity kaon decay experiment and carries out a broad rare-decay and hidden-sector physics program. In this talk, recent NA62 results on searches for violation of lepton flavour and lepton number in kaon decays, and searches for production of hidden-sector mediators in kaon decays, are presented. Future prospects of these searches are discussed. Searches for visible decays of exotic mediators from data taken in “beam-dump” mode with the NA62 experiment are also reported. The NA62 experiment can be run as a “beam-dump experiment” by removing the kaon production target and moving the upstream collimators into a “closed” position. More than 10^{17} protons on target have been collected in this way during a week-long data-taking campaign by the NA62 experiment. We report on new results from analysis of this data, with a particular emphasis on Dark Photon and Axion-like particle Models.

The future availability of high-intensity kaon beams at the CERN SPS North Area gives rise to unique possibilities for sensitive tests of the Standard Model in the kaon sector. An overview of the physics goals, detector requirements, and project status for HIKE, the next generation of kaon physics experiments at CERN, will be also presented.

Contents

1	The ultra-rare $K^+ \rightarrow \pi^+ \nu \bar{\nu}$ decay to probe Standard Model	4
2	$K^+ \rightarrow \pi^+ \gamma \gamma$ decay to probe ChPT predictions and search for axion-like particles	5
3	Search for HNL, DarkPhoton, ALPs	6
4	Current status of the NA62 and prospects for the future	8

Introduction

The NA62 is the currently operating fixed-target experiment located in the CERN North Area to measure the branching ratio of the ultra-rare $K^+ \rightarrow \pi^+ \nu \bar{\nu}$ decay with 10% precision. The experiment is working with the non-separated 75 GeV/c secondary hadron beam with the nominal beam intensity of 750 MHz and the average spill duration is 3.5 s. The beam is composed of 70 % protons, 24% π^+ and 6% K^+ . The current detector layout is present in Fig. 1.

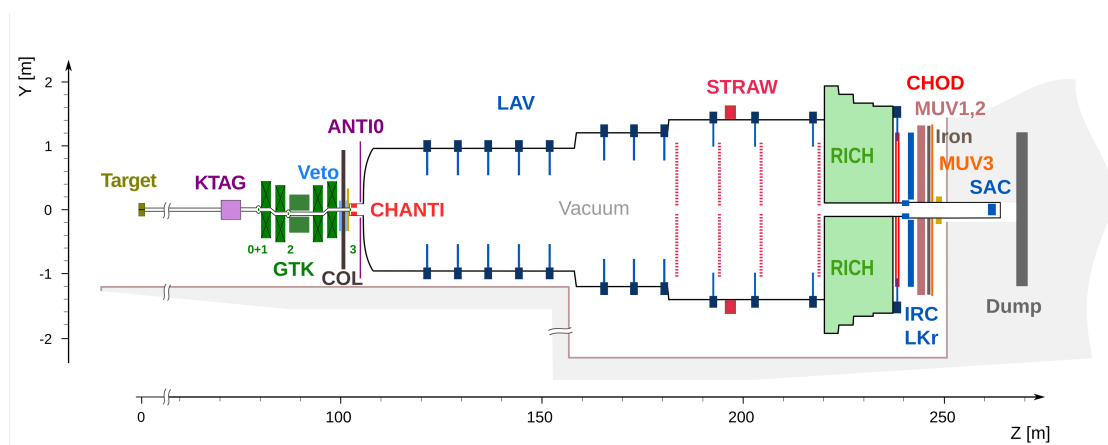


Figure 1: The NA62 detector layout

Kaons are produced after impinging the 400 mm long Beryllium target with the primary 400 GeV/c beam extracted from the SPS. The secondary hadron beam with the average momentum of 75 GeV/c is transported by the K12 beamline towards the ECN3 experimental hall where NA62 is hosted. The beam kaons are identified by the differential Cherenkov detector (KTAG) and their momentum is measured by the beam spectrometer (GTK). The Fiducial decay volume starts 105 meters downstream of the target and is equipped with the photon veto system (large angle veto, LAV). The momentum of the particles produced in the kaon decays is measured by the main spectrometer (STRAW), while particles are identified using RICH, fast muon hodoscope MUV3

and calorimeters (liquid Krypton electromagnetic calorimeter LKr and two hadron calorimeters MUV1 and MUV2). Charged particle hodoscope CHOD is used to generate a multiplicity trigger. All subsystems upstream of the RICH are located in the $O(10^{-6})$ vacuum. CHANTI suppresses background particles originating from the K and π decays upstream. There are a few new additions to the setup: ANTI-0 and VetoCounters (Veto) were installed during the CERN Long Shutdown 2 (2019 – 20) and additional copper collimator (COL) in 2018. One nominal year of operation is equal to 10^{18} POT (protons on target) or 4×10^{12} K^+ decays in the fiducial volume. The detailed description of the NA62 detector and the K12 beamline configuration is presented in [1]. Thanks to the multi-stage trigger system and several trigger lines used a large number of additional reactions could be studied in parallel with the main mode. Additionally, the detector layout allows performing studies in the so-called “beam-dump“ mode to search for weakly-coupling particles [2] which might be produced by the interaction of the primary beam with the material of the dump.

1. The ultra-rare $K^+ \rightarrow \pi^+ \nu \bar{\nu}$ decay to probe Standard Model

The $K^+ \rightarrow \pi^+ \nu \bar{\nu}$ decay proceeds through the electroweak box and penguin diagrams, both dominated by a t-quark exchange. It is highly suppressed due to the quadratic Glashow-Iliopoulos-Maiani (GIM) mechanism and the transition from a top to a down quark. The SM predicts the branching ratio to be $BR_{SM} = (8.60 \pm 0.42) \times 10^{-11}$ [3], where the uncertainty is dominated by the CKM parameters V_{cb} and γ . This makes $K^+ \rightarrow \pi^+ \nu \bar{\nu}$ an excellent process to probe for the evidence of the New Physics.

The 4-momentum of the beam K^+ , the 4-momentum of the secondary π^+ , and missing energy in the final state are the main kinematic variables used to define the two signal regions (Region 1 and Region 2) and several Control regions to separate $K^+ \rightarrow \pi^+ \nu \bar{\nu}$ and other decays. Reconstructed missing mass as a function of π^+ momentum without applying photon rejection and π^+ identification is shown in fig. 2 (left). The kinematic space is subdivided into two signal regions (Region 1 and Region 2) and control regions. A similar plot with experimental points obtained after analysing the 2018 data sample is present in Fig. 2(right).

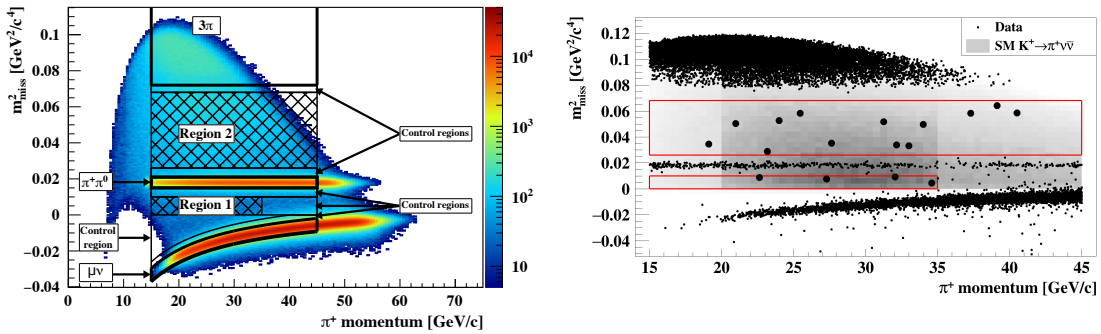


Figure 2: Reconstructed missing mass as a function of π^+ momentum. MC events with region definition (left) and with experimental points from 2018 data (right).

The integrated RUN1 (2016–2018) dataset collected for the $K^+ \rightarrow \pi\nu\bar{\nu}$ decay analysis contains 2.7×10^{12} kaon decays in the fiducial region with the single event sensitivity $= (0.839 \pm 0.053_{syst}) \times 10^{-11}$. In total 20 reconstructed $K^+ \rightarrow \pi^+\nu\bar{\nu}$ candidates were observed with the total number of expected signal events $N_{signal} = 10.01 \pm 0.42_{syst} \pm 1.19_{ext}$ and number of expected background events $N_{bkgd} = 7.03^{+1.05}_{-0.82}$. The measured value of the $K^+ \rightarrow \pi^+\nu\bar{\nu}$ branching ratio is:

$$\text{BR}(K^+ \rightarrow \pi^+\nu\bar{\nu}) = (10.6^{+4.0}_{-3.4}|_{\text{stat}} \pm 0.9|_{\text{syst}}) \times 10^{-11} \quad [4].$$

2. $K^+ \rightarrow \pi^+\gamma\gamma$ decay to probe ChPT predictions and search for axion-like particles

The experimental studies of radiative non-leptonic kaon decays allow to probe chiral perturbation theory predictions. Two kinematic variables (y, z) and a free parameter \hat{c} are used to describe the $K_{\pi\gamma\gamma}$ differential decay rate: $z = \frac{(q_1+q_2)^2}{m_K^2} = \left(\frac{m_{\gamma\gamma}}{m_K}\right)^2$, $y = \frac{p(q_1-q_2)}{m_K^2}$, where q_1, q_2 are 4-momenta of the photons, m_K and p are mass and four-momenta of the kaon, $m_{\gamma\gamma}$ – di-photon invariant mass. The calculations are described in [6]. The value of the \hat{c} parameter could be determined from the shape of the differential decay rate distribution. The $K \rightarrow \pi\gamma\gamma$ decay has no tree-level $O(p^2)$ contribution. The shape of the distribution is sensitive to the \hat{c} parameter and gives a lower limit: $\text{BR}(K^\pm \rightarrow \pi^\pm\gamma\gamma) \geq 4 \times 10^{-7}$

The selected data sample contains $N_K = 5.55 \pm 0.03 \times 10^{10}$ of kaon decays in the fiducial volume. The resulting 3984 $K^+ \rightarrow \pi^+\gamma\gamma$ decay candidates are selected after applying all the selection criteria including kinematic region cut $z = (P_K - P_\pi)/m_K^2 \equiv m_{\gamma\gamma}^2/m_K^2 > 0.2$. The number of background events is estimated as 291 ± 14 .

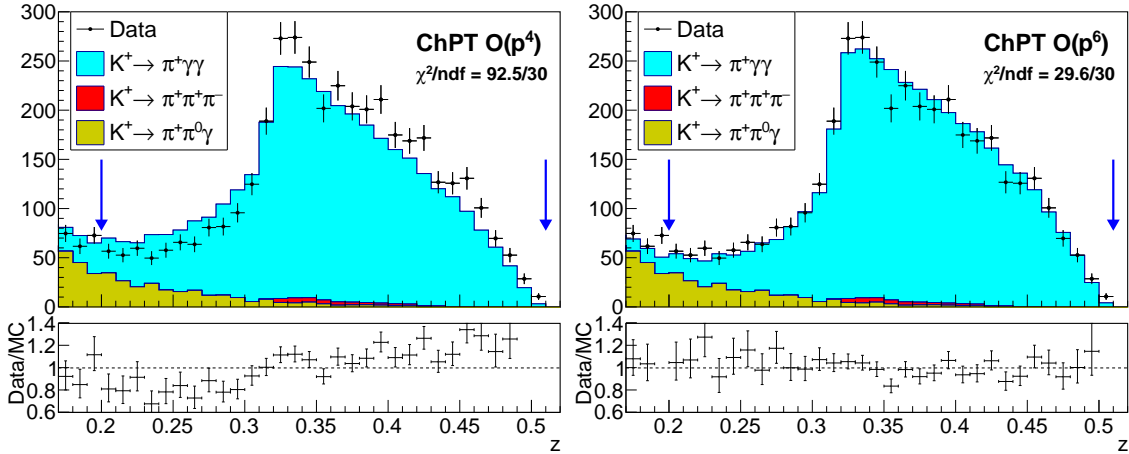


Figure 3: Reconstructed z spectrum of the $K^+ \rightarrow \pi^+\gamma\gamma$ candidates using $O(p^4)$ and $O(p^6)$ signal descriptions.

The obtained \hat{c} parameter used in the ChPT $O(p^6)$ description is found to be $\hat{c} = 1.144 \pm 0.069_{stat} \pm 0.034_{syst}$. The branching ratio obtained by integration of the ChPT $O(p^6)$ is $\text{BR}(K^\pm \rightarrow \pi^\pm\gamma\gamma) = (9.61 \pm 0.15_{stat} \pm 0.07_{syst}) \times 10^{-7}$.

Additionally, the result of the $\text{BR}(K^+ \rightarrow \pi^+\gamma\gamma)$ could be reinterpreted in terms of the search for the axion-like particle (ALP, a) $K^+ \rightarrow \pi^+a, a \rightarrow \gamma\gamma$. Under the assumption of $a \rightarrow \gamma\gamma$ decay, a mass from 207 to 350 MeV/ c^2 and decay time not exceeding 3 ns. An upper limit of the branching

ratio is evaluated for each axion mass hypothesis. The exclusion plot is present in fig.4. A detailed description of the analysis is published in [5].

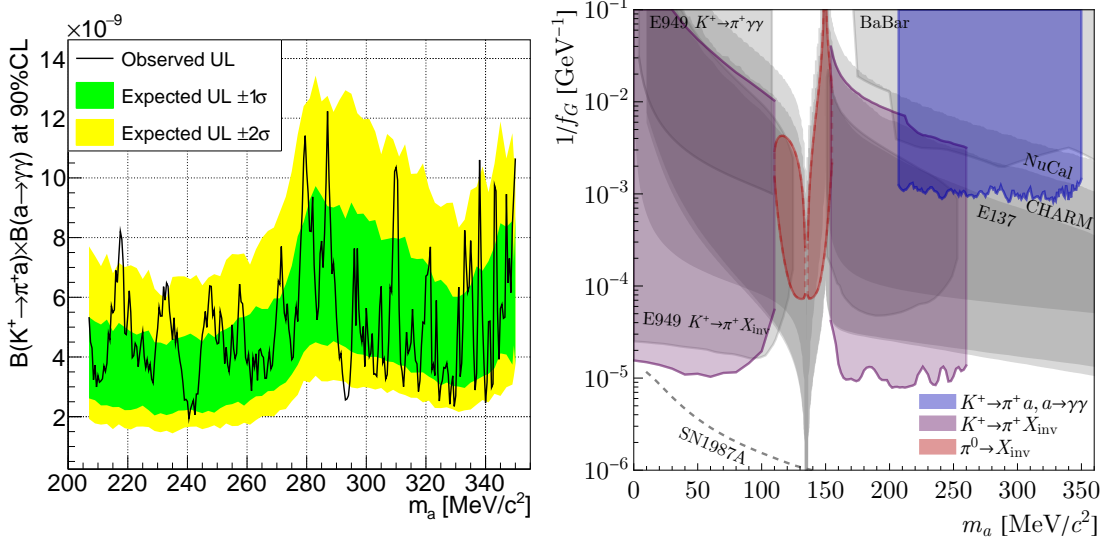


Figure 4: Upper Limit at 90% CL of $\text{BR}(K^\pm \rightarrow \pi^\pm a) \times \text{BR}(a \rightarrow \gamma\gamma)$ in the prompt decay assumption (left) and Limits obtained from the present $K^\pm \rightarrow \pi^\pm a, a \rightarrow \gamma\gamma$ decay, earlier NA62 searches ([4], [7]) and other experimental limits [8] in grey colour (right).

3. Search for HNL, DarkPhoton, ALPs

Kaon mode

The massive neutrinos, or heavy neutral leptons (HNLs), are described in various SM extensions. For example, the Neutrino Minimal Standard Model [9] predicts two HNLs in the MeV–GeV mass range and a third one at the keV mass scale. Precise measurements of the kaon decays allow to search for the HNL production in the mass range up to the kaon mass ($490 \text{ MeV}/c^2$). Using the entire Run 1 data sample the following searches have been performed: $K^+ \rightarrow \mu N$ and $K^+ \rightarrow \mu \nu N$ [11] and $K^+ \rightarrow e N$ [12]

Studies were performed with the assumption that an HNL lifetime exceeds 50 ns and there are no extra SM particles produced inside the NA62 detector – only one charged particle in the final state registered (e^+ or μ^+). The main kinematic parameter is the squared missing mass $m_{\text{miss}}^2 = (P_K - P_l)^2$, where P_K and P_l are the kaon and lepton 4-momenta, obtained from the 3-momenta measured by the GTK and STRAW spectrometers and K^+ and l^+ ($l = e, \mu$) mass hypotheses.

The main background contribution for the muon mode is coming from the $K^+ \rightarrow \mu^+ \nu_\mu \gamma$, $K^+ \rightarrow \mu^+ \nu_\mu \pi^0$ and $K^+ \rightarrow \pi^+ \pi^+ \pi^-$ decays. The background for mode with electrons in the final state is coming from $K^+ \rightarrow \mu^+ \nu$, $\pi^+ \rightarrow e^+ \nu_e$ and $\pi^+ \rightarrow \mu^+ \nu_\mu$ decays.

The summary plot with U_{e4} (electron-HNL mixing parameter) and $U_{\mu 4}$ (muon to HNL mixing parameter) as a function of HNL mass is shown in fig. 5.

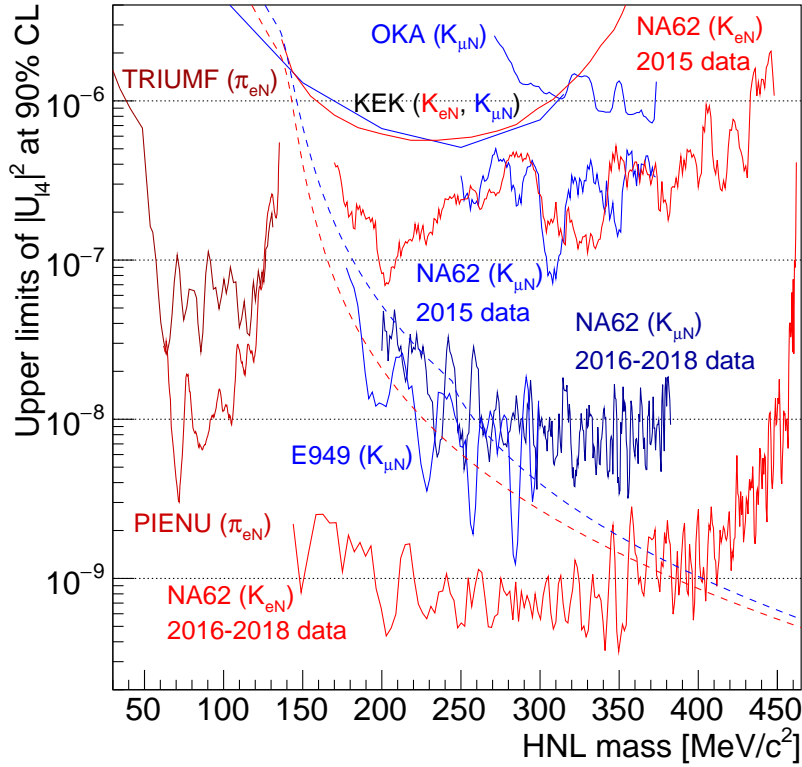


Figure 5: Mixing parameter upper limit as a function of HNL mass for electrons to HNL U_{e4} (red) and muons to HNL $U_{\mu 4}$ (blue).

Dump mode

The NA62 detector can operate in the beam-dump configuration. In this case, the Beryllium target is removed and the primary 400 GeV/c proton beam is stopped by collimators, which are switched in closed mode. Collimators are located about 45 m upstream of the KTAG and act as a beam dump. Typical beam intensity during the beam-dump mode is about 60×10^{11} protons per spill. In this configuration, the particle rate in the detectors downstream of the fiducial volume is of the order of 300 kHz, dominated by muons produced in the beam dump.

A possible dark photon can be emitted via a bremsstrahlung process ($\gamma^* p \rightarrow A' p'$) or as a product of intermediate meson decay ($pN \rightarrow MX$, where $M = \pi^0, \eta', \rho, \omega, \dots$) produced after initial proton interaction with the material of the dump. The search is performed assuming decay of $A' \rightarrow \mu^+ \mu^-$ and $A' \rightarrow e^+ e^-$ within the NA62 fiducial volume.

During the 2021 data-taking, the first year after LS2, the dedicated period of ~ 10 effective days for the beam-dump mode measurements was allocated. Three trigger lines with L0-trigger conditions were used:

- Q1/20 – trigger for the events with at least one signal in the CHOD and downscaled by a factor of 20;
- H2 – triggered by events with at least two in-time signals in two different tiles of the CHOD;

- E1 –selecting events with more than 1 GeV energy deposited in the LKr and at least one reconstructed LKr cluster.

The approximate rate for the trigger lines used was: 14 kHz for Q1/20, 18 kHz for H2 and 4 kHz for E1 trigger lines. The collected data sample corresponds to $\sim 1.4 \times 10^{17}$ dumped protons on target.

Two oppositely charged tracks that form a vertex within the NA62 fiducial volume are selected. Particle identification is based on the LKr and MUV3 responses. The additional veto conditions for in-time activities in LAV are applied to reduce the background of the secondary interactions of muons. A primary vertex is reconstructed as a minimum distance of approach between the total momentum of the di-muon pair and the nominal proton beam direction. Both a signal region (SR) and a control region (CR) are defined in the plane between the longitudinal position of the primary vertex. The excluded region for the coupling parameter ϵ as a function of A' mass ($M_{A'}$) is presented in Fig. 6.

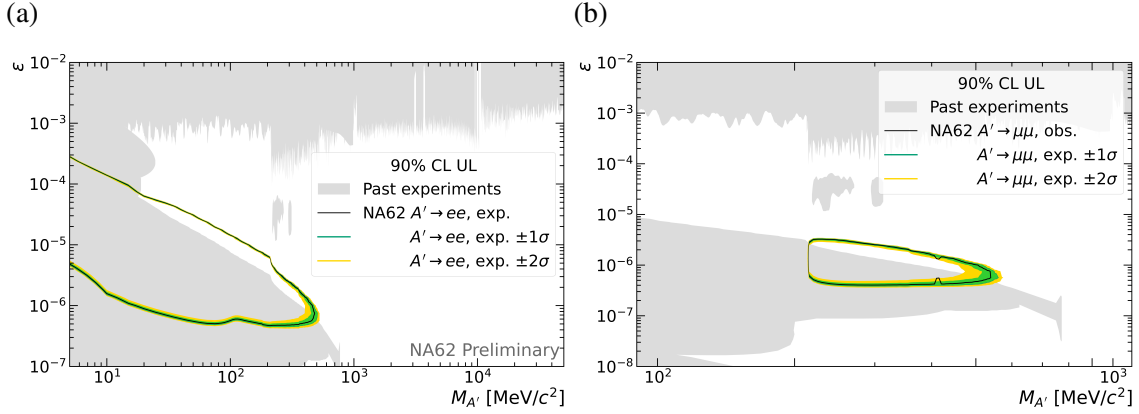


Figure 6: The mixing parameter ϵ as a function of A' mass for the decay $A' \rightarrow e^+e^-$ (left) and $A' \rightarrow \mu^+\mu^-$ (right). The solid line is excluded at 90% CL. The green and yellow areas represent the expected exclusion uncertainty within $\pm 1\sigma$ or $\pm 2\sigma$.

4. Current status of the NA62 and prospects for the future

The NA62 is a successfully operating experiment allowing to perform studies of the kaon decays with the single event sensitivity down to the level of $\sim 10^{-12}$.

Present experiment configuration allows to perform various studies in parallel to the main $K^+ \rightarrow \pi^+\nu\bar{\nu}$ mode, including searches for lepton flavor and lepton number violating decays [13], [14], [15] and precise measurements of the rare decay properties [16],[17].

In 2023 the proposal to extend Kaon physics at CERN to a new level of sensitivity has been published as the new multi-phase experiment–High-Intensity Kaon Experiment (HIKE) [18].

HIKE Phase One – an improved version of the present experimental layout, that allows operating with 4 times higher beam intensity to reach 5% precision in the $K^+ \rightarrow \pi^+\nu\bar{\nu}$ measurements in a reasonable amount of operational years. This phase allows for significant improvement in the precision of all existing measurements of the K^+ decays. Some changes in the hardware part and the development of a new readout system are required, while almost the whole infrastructure, except

the beamline and target complex, might be inherited from the NA62. The schematic layout of the HIKE experiment during Phase 1 is shown in fig. 7.

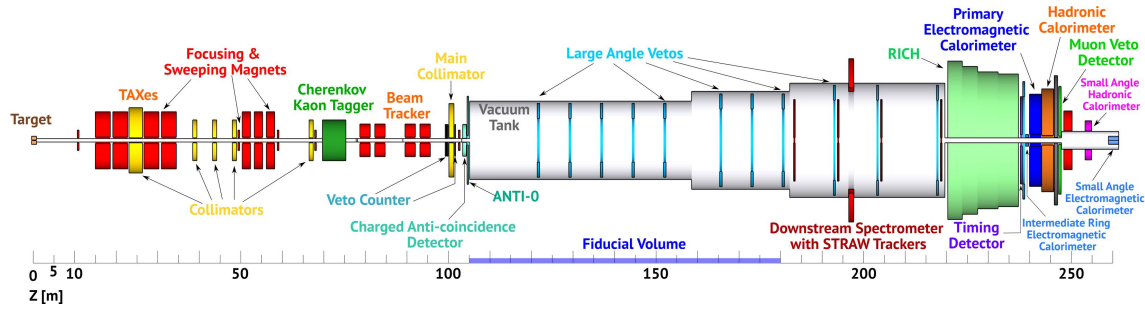


Figure 7: Schematic layout of the HIKE experimental setup during phase 1 (charged Kaon mode)

HIKE Phase Two (schematic layout is shown in fig. 8) changes experimental focus from charged to neutral kaon mode to study K_L decays with the new level of precision. Measurements of the $K_L \rightarrow \pi\nu\bar{\nu}$ decay are going to be discussed later within the HIKE phase 3. During the second phase, some significant changes in the K12 beamline and the removal of some subdetectors are foreseen. Additionally the start of the fiducial volume and main spectrometer position are to be moved several meters downstream, while the position of all the calorimeters remains the same.

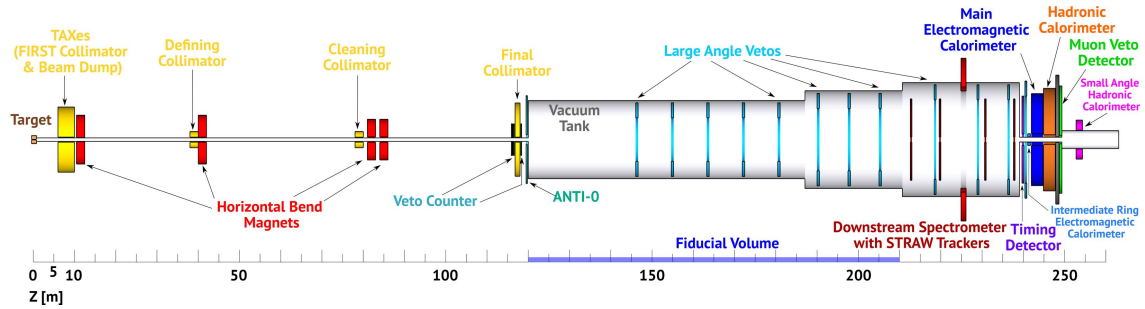


Figure 8: Schematic layout of the HIKE experimental setup during phase 2 (neutral mode).

There is another experiment aiming to be located at the same time and in the same experimental hall. The decision on the future frontline experiment in the CERN North Area is expected to be taken in the first half of 2024.

References

- [1] JINST **12** (2017) no.05, P05025
- [2] B. Döbrich [NA62], [arXiv:1711.08967 [hep-ex]].
- [3] A. J. Buras, [arXiv:2307.15737 [hep-ph]].
- [4] JHEP **06** (2021), 093
- [5] [arXiv:2311.01837 [hep-ex]].

- [6] G. Ecker, A. Pich and E. de Rafael, Nucl. Phys. B **303**, 665 (1988).
- [7] JHEP **02** (2021), 201
- [8] M. W. Winkler, Phys. Rev. D **99** (2019) no.1, 015018
- [9] T. Asaka and M. Shaposhnikov, Phys. Lett. B **620** (2005), 17-26
- [10] Phys. Lett. B **807** (2020), 135599
- [11] Phys. Lett. B **816** (2021), 136259
- [12] Phys. Lett. B **807** (2020), 135599
- [13] Phys. Lett. B **838** (2023), 137679
- [14] Phys. Lett. B **830** (2022), 137172
- [15] Phys. Lett. B **797** (2019), 134794
- [16] JHEP **11** (2022), 011
- [17] JHEP **09** (2023), 040
- [18] M. U. Ashraf *et al.* [HIKE], [arXiv:2311.08231 [hep-ex]].